PERGAMON

International Journal of Solids and Structures 38 (2001) 5165–5183

INTERNATIONAL JOURNAL OF SOLIDS and STRUCTURES

www.elsevier.com/locate/ijsolstr

Optimal truss plates

Nathan Wicks, John W. Hutchinson *

Division of Engineering and Applied Sciences, 315, Pierce Hall, Harvard University, 29 Oxford Street, Cambridge, MA 02138, USA

Received 23 March 2000; in revised form 3 August 2000

Abstract

Sandwich plates comprised of truss cores faced with either planar trusses or solid sheets are optimally designed for minimum weight subject to prescribed combinations of bending and transverse shear loads. Motivated by recent advances in manufacturing possibilities, attention is focussed on plates with truss elements and faces made from a single material. The optimized plates are compared with similarly optimized honeycomb core sandwich plates fashioned from the same material. Sandwich plates with solid sheet faces and truss cores are highly efficient from a weight standpoint. These are also studied for their performance as compression panels. Optimized compression panels of this construction compare favorably with the most efficient stringer stiffened plates.

Keywords: Truss plates; Octet truss; Optimal design

1. Introduction

Recent developments in the manufacturing of truss structures appear to greatly extend their application possibilities. New efficient casting-based procedures have been devised which permit entire truss structure components to be produced at scales ranging from millimeters to tens of centimeters. Two examples are shown in Fig. 1. Electro-deposition has been used to form truss structures at an even smaller scales with elements whose diameters can be as small as fifty microns (Brittain et al., 2000). Efforts are underway to determine the stiffness of truss structures and to assess their strength, both experimentally and theoretically (Wallach and Gibson, 2000).

Well designed structures using truss elements can be highly efficient from a weight standpoint, as will be established for plates in this paper. They have additional potential by virtue of their open structure for multi-functional applications. For example, sandwich plates with solid skins and truss cores can serve as a heat transfer elements simultaneously carrying loads. The cavity between the skins could be used for storage of a liquid or pressurized gas in other applications. Honeycomb core sandwiches or conventional stringer stiffened construction does not facilitate either of these dual purposes.

* Corresponding author. Tel.: +1-617-495-2848; fax: +1-617-495-9837.
E-mail address: hutchinson@husm.harvard.edu (J.W. Hutchinson).

0020-7683/01/$ - see front matter
PII: S0020-7683(00)00315-2

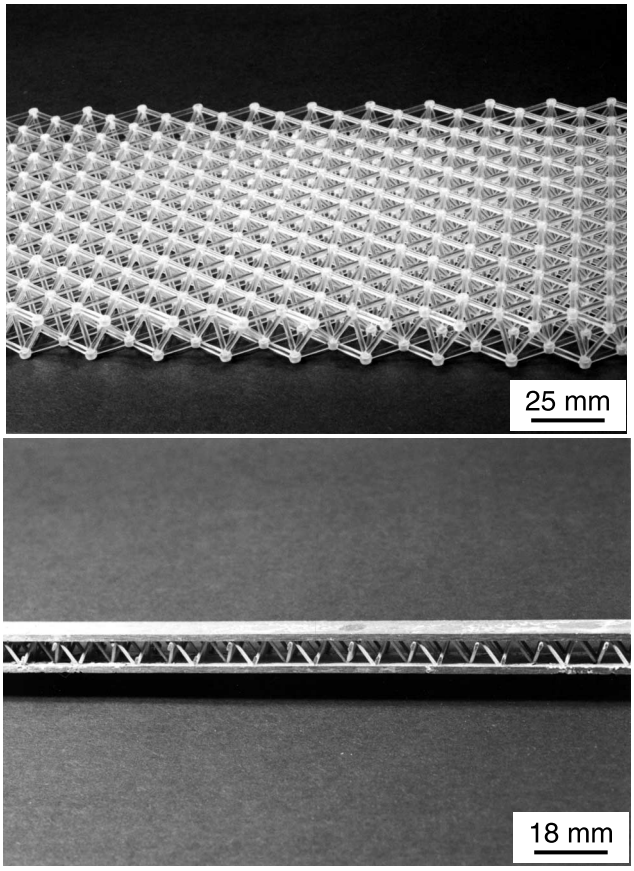

Fig. 1. Sandwich plates. Octet truss plate whose members are identical (top) and sandwich plate with truss core (bottom).

The two types of plate structures considered in this paper are shown in Fig. 2. One has triangulated planar truss faces, while the other has solid sheet faces. Each has a truss core with 120° in-plane symmetry. The plates are uniform (untapered). The length of the members in the core is L_c and the core thickness is H_c. The angle between the core members and the faces is $\varphi_c = \sin^{-1}(H_c/L_c)$. In the present study, only solid circular members will be considered, and the core member radius is R_c. For the plates with truss faces (Fig. 2a), the length and radius of the solid circular face members are denoted by L_f and R_f where,

$$L_f = \sqrt{3(L_c^2 - H_c^2)}. \tag{1}$$

The thickness of the solid isotropic sheets comprising the faces of the sandwich plates in Fig. 2b is denoted by t_f. The 120° symmetry of the plates ensures that their bending and in-plane stretching stiffnesses are isotropic.

While more efficient designs might make use of distinct materials for the core and faces, here we will limit the possibilities by taking a common material for all truss members and face sheets. The Young's modulus, Poisson's ratio, uniaxial yield strength and weight density of the material are denoted by E, ν, σ_Y and ρ, respectively. The designs will account for buckling and plastic yielding of the faces and core members. Optimal designs will be sought, wherein the weight is minimized subject to the failure constraints for

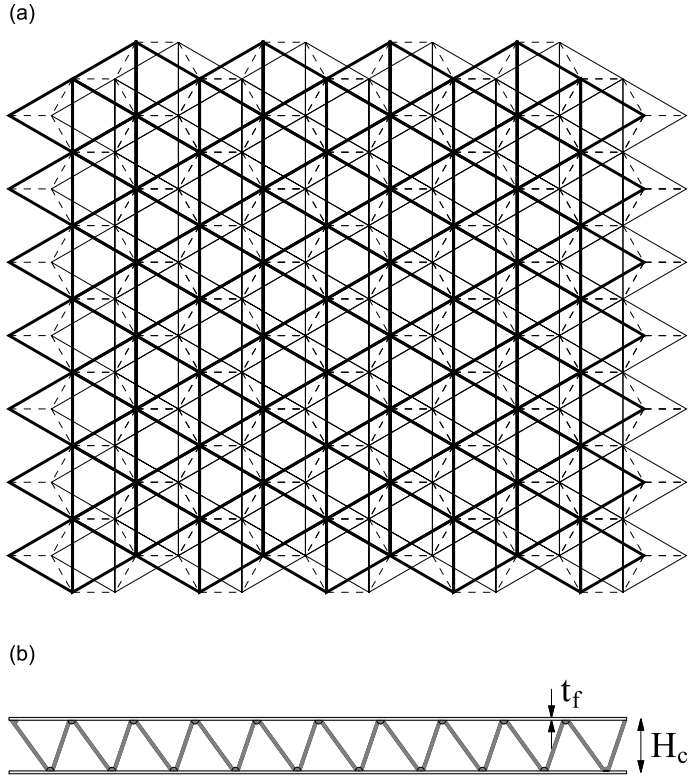

Fig. 2. Plate structures with truss cores. (a) Plates with planar truss faces. The darker members are top face members, the lighter solid members the bottom face members, and the dashed members the core members. (b) Plates with solid sheet faces.

specified combinations of bending moment and transverse shear force. In addition, optimal design of the plates as compression panels will be considered. The weight per unit area of the plate with truss faces is

$$W = 2\sqrt{3}\pi\rho\left[2\frac{R_f^2}{L_f} + \frac{L_c R_c^2}{L_f^2}\right], \tag{2}$$

and that of the plate with solid sheet faces is

$$W = 2\rho\left[t_f + \frac{\pi}{\sqrt{3}}\frac{L_c R_c^2}{L_c^2 - H_c^2}\right]. \tag{3}$$

2. Plates with truss cores and truss faces subject to bending and transverse shear

The general situation envisioned for the design problem is that the uniform, infinitely wide plate must carry a maximum moment per unit length M and a maximum transverse shear force per unit length V. Bending occurs only about the direction parallel to the loading line. A wide plate under three-point loading, with force per unit length, $2P$, at the center is a prototypical example. Each half of the plate carries a uniform transverse shear load per length, $V = P$, and a maximum moment per length, $M = P\ell$, at the

center, where ℓ is the half-length of the plate. In this example, the maximum moment and the maximum shear transverse force are attained at the same point, but that is not essential nor to be expected. In the general situation, the ratio of the maximum moment to the maximum transverse force (both per unit length),

$$\ell \equiv \frac{M}{V}, \tag{4}$$

defines a quantity with dimensions of length which will be central in the analysis. The study is limited to relatively thin plates in the sense that the thickness, H_c, is assumed to be small compared to ℓ. Thus, L_c/ℓ and L_f/ℓ will also be small.

An essential step in the optimization process is the determination of the maximum member forces in terms of maximum moment and maximum shear force. To facilitate the analysis, the truss joints are idealized as pin joints offering no rotational resistance from member to member or to the faces. The member forces are expected to be given fairly accurately by this idealization, which is widely used in truss analysis. However, the buckling resistance of the truss will be underestimated, thereby overestimating the weight of the optimal structure. Implications of the assumption of pinned joints will be discussed later in the paper.

The truss plate of Fig. 2(a) is not statically determinant: for each repeating unit of the structure there are three more unknown member forces than joint equilibrium equations. Nevertheless, simple expressions for member forces can be obtained from equilibrium considerations alone for certain load orientations. For the load orientation parallel to A–A' in Fig. 3, the deformation involves bending about a single direction (A–A'), assuming appropriate constraint at infinity in the transverse direction. The members in the faces parallel to the load line undergo no straining and their forces are zero. The remaining member forces can be obtained

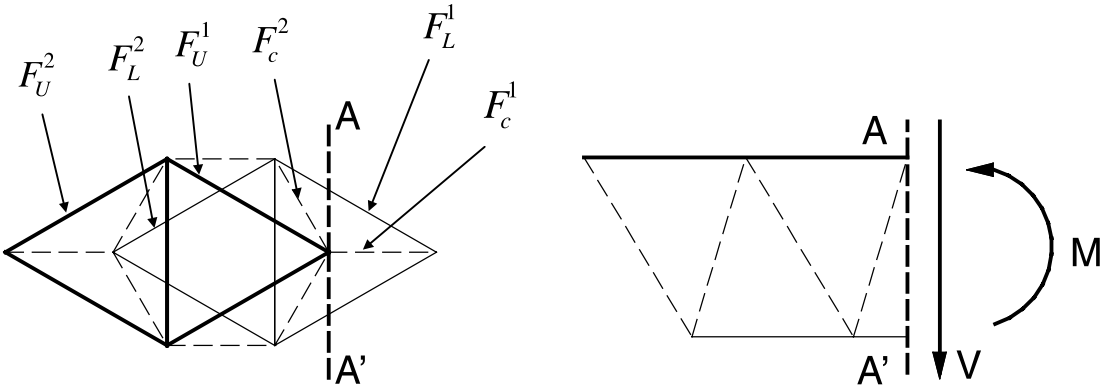

$$F_c^1 = -VL_f\left(\frac{L_c}{H_c}\right) \qquad F_c^2 = \frac{VL_f}{2}\left(\frac{L_c}{H_c}\right)$$

$$F_U^1 = \frac{ML_f}{\sqrt{3}}\left(\frac{1+\left(\frac{L_f}{l}\right)\frac{1}{2\sqrt{3}}}{H_c}\right) \qquad F_U^2 = \frac{ML_f}{\sqrt{3}}\left(\frac{1+\left(\frac{L_f}{l}\right)\frac{2}{\sqrt{3}}}{H_c}\right)$$

$$F_L^1 = -\frac{ML_f}{\sqrt{3}H_c} \qquad F_L^2 = -\frac{ML_f}{\sqrt{3}}\left(\frac{1+\left(\frac{L_f}{l}\right)\frac{\sqrt{3}}{2}}{H_c}\right)$$

Fig. 3. Nonzero member forces in the truss plate at section A–A'. The load line is parallel to A–A', and the members which are parallel to A–A' carry zero force.

from the method of sections. Consider a typical section A–A' shown in Fig. 3, where the moment per unit length and transverse force per unit length carried by the plate at that section are M and V. The members with nonzero forces are labeled in Fig. 3. The method of sections gives the member forces neighboring A–A', as detailed in Fig. 3. The forces in the core members are

$$F_c^1 = -VL_f\left(\frac{L_c}{H_c}\right), \qquad F_c^2 = \frac{VL_f}{2}\left(\frac{L_c}{H_c}\right). \tag{5}$$

If terms of relative order L_f/ℓ are neglected in the expression for the force in the face members, the members inclined to the load line experience

$$F_f = \frac{M}{\sqrt{3}}\left(\frac{L_f}{H_c}\right) \tag{6}$$

with due account for the sign difference between the top and bottom members. Forces in all the other members can be derived from these formulas by accounting for the shift of M and V from section to section.

The magnitude of the maximum force in a core member is thus related to the *maximum* shear force per unit length, V, by

$$F_c = VL_f\left(\frac{L_c}{H_c}\right). \tag{7}$$

This force is compressive if V acts downward in Fig. 3, which will be assumed in the following. (Note, for example, that the truss in a three-point bend configuration experiences a sign of V on one side of the center and the opposite sign on the other. In this case, therefore, the maximum compressive load in a core member is always Eq. (7)). Let the *maximum* moment per unit length be M, it follows that the magnitude of the maximum force in a face sheet member is

$$F_f = \frac{M}{\sqrt{3}}\left(\frac{L_f}{H_c}\right), \tag{8}$$

acting as compression in one of the faces and tension in the other, depending on the sense of M.

The four constraints on the maximum member forces are

$$\frac{M}{\sqrt{3}}\left(\frac{L_f}{H_c}\right) \leqslant \sigma_Y \pi R_f^2, \text{ (face member yielding)}, \tag{9a}$$

$$\frac{M}{\sqrt{3}}\left(\frac{L_f}{H_c}\right) \leqslant \frac{\pi^3 E R_f^4}{4L_f^2}, \text{ (face member buckling)}, \tag{9b}$$

$$VL_f\left(\frac{L_c}{H_c}\right) \leqslant \sigma_Y \pi R_c^2, \text{ (core member yielding)}, \tag{9c}$$

$$VL_f\left(\frac{L_c}{H_c}\right) \leqslant \frac{\pi^3 E R_c^4}{4L_c^2}, \text{ (core member buckling)}. \tag{9d}$$

The two conditions on buckling take the beam members to be simply-supported at their ends, consistent with the pinned joint idealization. In each case, this approximation provides a lower bound to the actual member forces which can be sustained. Later in the paper, we will provide some indication of the extent to which the underestimate of the critical buckling loads affects the optimization outcome. Improvement of the present analysis will require more accurate formulas for the buckling constraints (9b) and (9d).

2.1. The optimization problem

The maximum load quantities, M and V, are assumed to be specified and ℓ is given by Eq. (4). The material properties are also specified. Define four dimensionless geometric design variables as

$$\vec{x} \equiv (x_1, x_2, x_3, x_4) = (R_f/\ell, L_f/\ell, R_c/\ell, H_c/\ell), \tag{10}$$

where $L_c/\ell = \sqrt{x_4^2 + x_2^2/3}$. The dimensionless weight per unit area of the truss plate from Eq. (2) is

$$\frac{W}{\rho\ell} = 2\sqrt{3}\pi\left[2x_1^2x_2^{-1} + x_3^2x_2^{-2}\sqrt{x_4^2 + x_2^2/3}\right]. \tag{11}$$

The optimization problem requires the minimization of $W/\rho\ell$ with respect to $\vec{x}$ subject to the four constraints in Eq. (9), which in dimensionless form become

$$\frac{1}{\sqrt{3}\pi}\left(\frac{V^2}{EM}\right)\left(\frac{E}{\sigma_Y}\right)x_1^{-2}x_2x_4^{-1} \leqslant 1, \text{ (face member yielding)}, \tag{12a}$$

$$\frac{4}{\sqrt{3}\pi^3}\left(\frac{V^2}{EM}\right)x_1^{-4}x_2^3x_4^{-1} \leqslant 1, \text{ (face member buckling)}, \tag{12b}$$

$$\frac{1}{\pi}\left(\frac{V^2}{EM}\right)\left(\frac{E}{\sigma_Y}\right)x_2x_3^{-2}x_4^{-1}\sqrt{x_4^2 + x_2^2/3} \leqslant 1, \text{ (core member yielding)}, \tag{12c}$$

$$\frac{4}{\pi^3}\left(\frac{V^2}{EM}\right)x_2x_3^{-4}x_4^{-1}\left(x_4^2 + x_2^2/3\right)^{3/2} \leqslant 1, \text{ (core member buckling)}. \tag{12d}$$

There is one dimensionless material parameter in the problem, σ_Y/E, and only one dimensionless load parameter, $V^2/(EM)$.

2.2. The optimal plate truss

The optimization problem has been solved using a sequential quadratic programming algorithm which is included in the IMSL Library. The material is assumed to be representative of a relatively high strength aluminum with $\sigma_Y/E = 0.007$. The optimization is carried out for specified values of $V^2/(EM)$. An effective parameter tracking method uses the solution at one value of $V^2/(EM)$ as the initial guess in the iteration for the solution at a smaller $V^2/(EM)$, because this guess necessarily satisfies all the inequalities in Eq. (12). The solution is presented in Figs. 4 and 5. Both the dimensionless weight parameter and the member geometry parameters are plotted against $V/\sqrt{EM}$, rather than $V^2/(EM)$, because the variations are nearly linear in $V/\sqrt{EM}$. The plots are terminated at $V/\sqrt{EM} \cong 0.002$. Larger values of $V/\sqrt{EM}$ would generate plates that would not be considered as thin. Over the entire range of $V/\sqrt{EM}$ plotted, three of the constraints in Eq. (12) are active: face member buckling and yielding, and core member buckling.

2.3. Optimal plate truss with identical face and core members

Consider a subset of truss plates, known as octet trusses (Fuller, 1983), comprised of identical members, i.e.,

$$R_f = R_c \equiv R, \quad L_f = L_c \equiv L, \quad \text{and} \quad H_c = \sqrt{2/3}L \tag{13a}$$

with

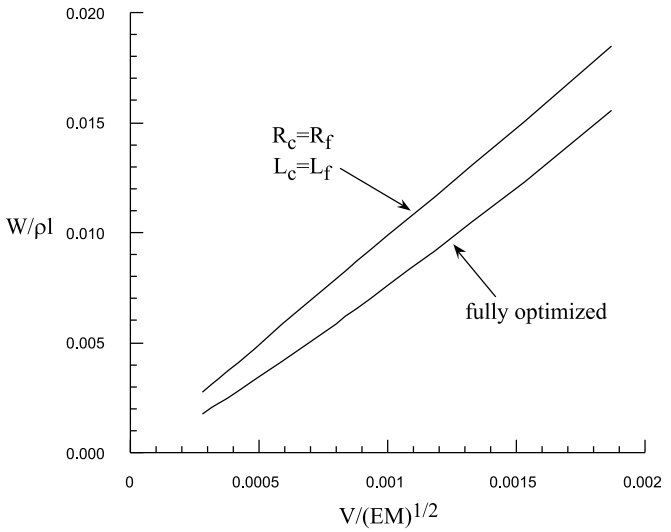

Fig. 4. Normalized weight per unit area of optimized truss plates as a function of the dimensionless load parameter ($\sigma_Y/E = 0.007$). The upper curve applies to an octet truss plate whose members are all the same. The lower curve is for a fully optimized truss plate with distinct face and core members.

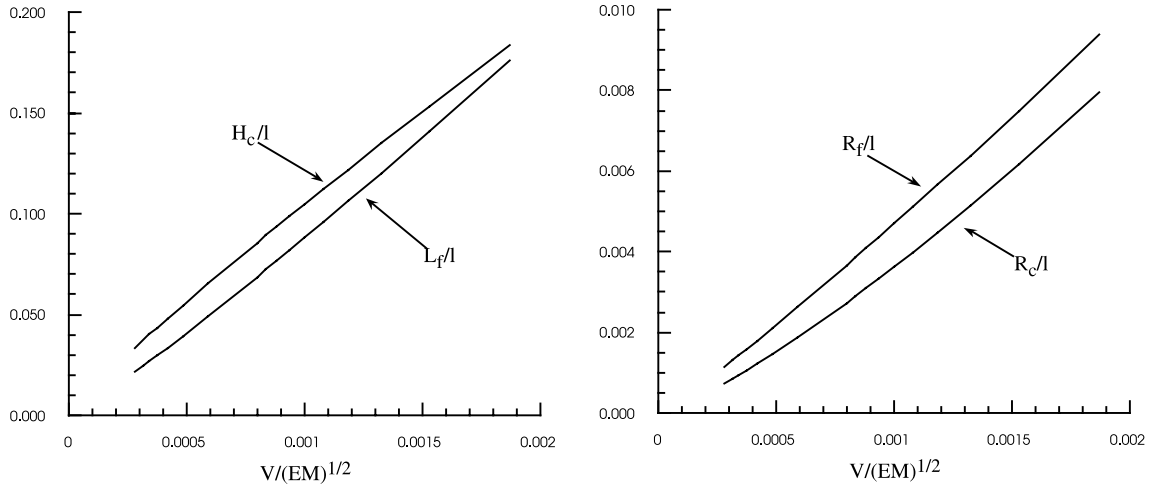

Fig. 5. Member sizes for the fully optimized truss plate, where $\ell = M/V$ ($\sigma_Y/E = 0.007$).

$$x_1 = R/\ell, \quad \text{and} \quad x_2 = L/\ell. \tag{13b}$$

This subset is interesting from the vantage point of its geometric aesthetics, and plate trusses in this class (Fig. 1) have been constructed in both plastic and metal. Eqs. (11) and (12) become

$$\frac{W}{\rho\ell} = 6\sqrt{3}\pi x_1^2 x_2^{-1}, \tag{14}$$

and

$$\frac{1}{\sqrt{2}\pi}\left(\frac{V^2}{EM}\right)\left(\frac{E}{\sigma_Y}\right)x_1^{-2} \leqslant 1, \text{ (face member yielding)}, \tag{15a}$$

$$\frac{2\sqrt{2}}{\pi^3}\left(\frac{V^2}{EM}\right)x_1^{-4}x_2^2 \leqslant 1, \text{ (face member buckling)}, \tag{15b}$$

$$\frac{\sqrt{3}}{\sqrt{2}\pi}\left(\frac{V^2}{EM}\right)\left(\frac{E}{\sigma_Y}\right)x_1^{-2}x_2 \leqslant 1, \text{ (core member yielding)}, \tag{15c}$$

$$\frac{2\sqrt{6}}{\pi^3}\left(\frac{V^2}{EM}\right)x_1^{-4}x_2^3 \leqslant 1, \text{ (core member buckling)}. \tag{15d}$$

Comparison of Eqs. (15a) and (15c) reveals that the core members will never yield before the face members if $\sqrt{3}x_2 < 1$, which will always pertain to slender plate trusses. Similarly, $\sqrt{3}x_2 < 1$ ensures that face member buckling will always precede core member buckling. Thus, only face member yielding and buckling need to be considered. Anticipate that face member buckling governs, i.e., from Eqs. (15a) and (15b):

$$x_1 \equiv \frac{R}{\ell} > \frac{1}{\sqrt{\sqrt{2}\pi}}\left(\frac{V}{\sqrt{EM}}\right)\sqrt{\frac{E}{\sigma_Y}}, \tag{16}$$

and

$$x_1^2 x_2^{-1} = \frac{2}{\sqrt{\sqrt{2}\pi^3}}\left(\frac{V}{\sqrt{EM}}\right). \tag{17}$$

Then one notes immediately from Eqs. (17) and (14) that the normalized minimum weight per unit area depends precisely linearly on $V/\sqrt{EM}$ according to

$$\frac{W}{\rho\ell} = \frac{12\sqrt{3}}{\sqrt{\sqrt{2}\pi}}\frac{V}{\sqrt{EM}} = 9.861\frac{V}{\sqrt{EM}}. \tag{18}$$

The minimum is attained for any *combination* of x_1 and x_2 satisfying Eq. (17) and $\sqrt{3}x_2 < 1$. Note also that if the equality in Eq. (16) is met together with Eq. (17), corresponding to simultaneous buckling and yielding of the face members, the minimum is still given by Eq. (18). Further inspection of the constraints reveals that if yield holds but buckling does not, then the normalized weight exceeds Eq. (18). It follows, for all $V/\sqrt{EM}$, the minimum weight is given by Eq. (18), since x_1 and x_2 can always be chosen to meet Eqs. (16) and (17). The minimum weight relation (18) for truss plates with identical members is included in Fig. 4, and it can be seen to lie between 20% and 30% above the minimum weight for the truss plates, whose core and face members are not constrained to be the same.

Minimum weight octet trusses with identical members are not unique. A *family of trusses* exists, specified by Eq. (17) and limited by Eq. (16), for which each truss is at minimum weight. A curious outcome of this nonuniqueness is that any plate truss whose members are identical is a minimum weight truss for some particular loading. More precisely, given a geometry specified by x_1 and x_2, determine $V/\sqrt{EM}$ from Eq. (17). If Eq. (16) is met, it follows that the truss is minimum weight at $V/\sqrt{EM}$.

With reference to the dimensional Eqs. (9a) and (9b), it can be seen that V plays no role in the optimization of the truss plate with identical members. The design of this restricted class of plates is, in effect, designed under a pure moment M. This is revealed by rewriting Eq. (18), with the aid of Eq. (4), as

$$\frac{W}{\rho} = \frac{12\sqrt{3}}{\sqrt{\sqrt{2}\pi}}\sqrt{\frac{M}{E}}. \tag{19}$$

For design under a pure moment per unit length, there is only one length quantity, $\sqrt{M/E}$. When the truss core members are design variables, the problem reverts to a problem depending on $V/\sqrt{EM}$, but not $\sqrt{M/E}$. At very low values of $V/\sqrt{EM}$, a long-wavelength buckling mode, akin to a plate buckling on an elastic foundation, must be considered. This mode brings in the length quantity $\sqrt{M/E}$ in addition to M/V. The regime in which this additional mode is important will be investigated in subsequent work.

3. Plates with truss cores and solid sheet faces subject to bending and transverse shear

Replace the face members in the truss plates just considered by solid sheets of thickness t_f of the same base material leaving the truss core unchanged. The weight per unit area of the resulting sandwich plate is given by Eq. (3), and the four design variables are t_f, R_c, H_c and L_c. As in the case of the truss plates, consider infinitely wide plates subject to line loads oriented relative to the truss core in the same manner considered before (Fig. 3), inducing bending about the direction parallel to A–A'. Let M and V be the maximum moment and shear force per unit length. The maximum stress in the face sheets and the maximum force in the truss members again can be obtained from elementary equilibrium using the method of sections, neglecting the small contribution from transverse shear stresses within the face sheets:

$$\sigma_f = \frac{M}{t_f H_c}, \quad F_c = \frac{\sqrt{3}VdL_c}{H_c}, \tag{20}$$

where $d \equiv \sqrt{L_c^2 - H_c^2}$. As is commonplace in the analysis of thin-skinned sandwich structures, the formula for σ_f neglects terms of relative order t_f/H_c under the assumption that $t_f/H_c \ll 1$. One face sheet experiences compression and the other, tension of the same magnitude. The sense of V is assumed to be such that the maximum truss member force in Eq. (20) is compressive, just as in the case of the analysis in Section 2.

The four failure modes taken into account in designing the optimal sandwich plate are face sheet yielding, face sheet buckling, core member yielding and core member buckling. The associated constraints are

$$\frac{M}{t_f H_c} \leqslant \sigma_Y, \text{ (face sheet yielding)}, \tag{21a}$$

$$\frac{M}{t_f H_c} \leqslant \frac{49\pi^2 E}{432(1-\nu^2)}\left(\frac{t_f}{d}\right)^2, \text{ (face sheet buckling)}, \tag{21b}$$

$$\frac{\sqrt{3}VdL_c}{H_c \pi R_c^2} \leqslant \sigma_Y, \text{ (core member yielding)}, \tag{21c}$$

$$\frac{\sqrt{3}VdL_c}{H_c \pi R_c^2} \leqslant \frac{k\pi^2 E R_c^2}{4L_c^2}, \text{ (core member buckling)}. \tag{21d}$$

The mode of face sheet buckling (or wrinkling) leading to Eq. (21b) is shown in Fig. 6. The skin is assumed to buckle with the node lines shown. The rotation restraining effect of the truss core on the face sheets at the points of attachment is neglected. Thus, Eq. (21b) is expected to underestimate somewhat the maximum moment at buckling. The factor k in Eq. (21d) will be adjusted to model different end conditions for core

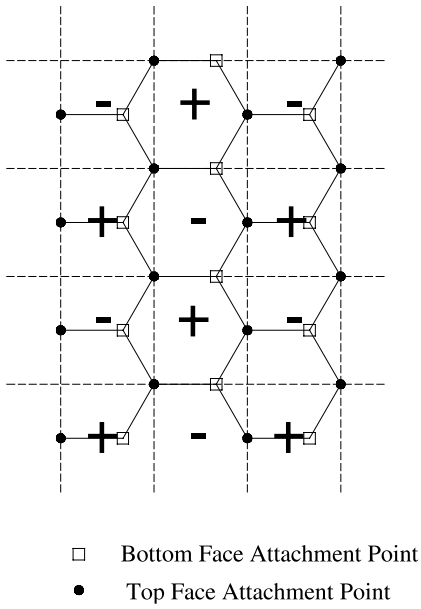

Fig. 6. Nodal lines of the face sheet buckling mode for sandwich plates with truss core. Compression is in the horizontal direction. A "+" within nodal lines represents an upward deflection, while a "−" denotes a downward deflection.

member buckling. The choice $k = 1$ corresponds to simply-supported conditions at the member ends. This choice, which will be used in most of the computations, neglects the rotational constraint provided by the other members and the face sheet at each end. This choice will certainly underestimate the maximum allowable shear force associated with core member buckling. The other extreme choice is $k = 4$, corresponding to fully clamped conditions at each end. This choice is expected to significantly overestimate the maximum shear force at buckling. Predictions based on the two limiting choices, $k = 1$ and 4, will be contrasted to assess the sensitivity to this constraint of the optimal design.

The weight per unit area (3) and the constraints (21) are written in dimensionless form using $\ell = M/V$ and the four design variables

$$\vec{x} = (t_f/\ell, R_c/\ell, H_c/\ell, d/\ell). \tag{22}$$

The normalized weight per unit area, $W/\rho\ell$, and the four dimensionless constraints involve only σ_Y/E (and ν, which is taken to be 1/3 in the calculations) and $V^2/(EM)$, as well as $\vec{x}$. For a given σ_Y/E, the relation of $W/\rho\ell$ to $V^2/(EM)$ is universal for the optimally designed sandwich plate. That relation is plotted in Fig. 7 over the range for which the plates can be considered slender or "thin" for $\sigma_Y/E = 0.007$ with $k = 1$. The associated values of the design variables are plotted in Fig. 8. The active constraints over the entire range plotted are face sheet yielding and buckling, and core member buckling. If the geometry of the core truss is constrained in the same manner as was considered of the octet trusses in Section 2, i.e., such that and $d = L_c/\sqrt{3}$, then there are only three independent design variables, t_f/ℓ, R_c/ℓ and H_c/ℓ. The optimal sandwich plate in this sub-class is also included in Fig. 7, where it can be seen to be only slightly heavier than the fully optimized structure. The important implication is that this special core geometry appears to be almost as promising as the fully optimized core. The same three constraints noted above are active.

As remarked above, the assumption of simply supported truss member ends ($k = 1$) is conservative, leading to an overestimate of $W/\rho\ell$. The effect of taking the end conditions to be fully clamped ($k = 4$) is

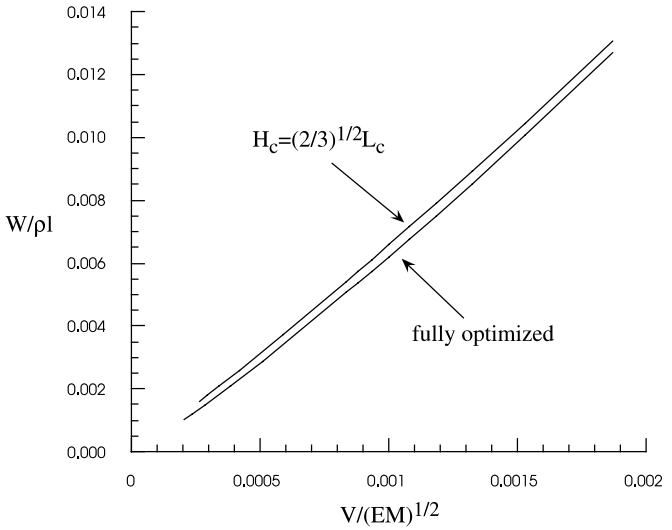

Fig. 7. Normalized weight per unit area as a function of the dimensionless load parameter for optimally designed sandwich plates with truss cores ($\sigma_Y/E = 0.007$, $\nu = 1/3$ and $k = 1$). The geometry of the plate for the upper curve is constrained such that $H_c = \sqrt{2/3}L_c$. The lower curve is for the fully optimized plate.

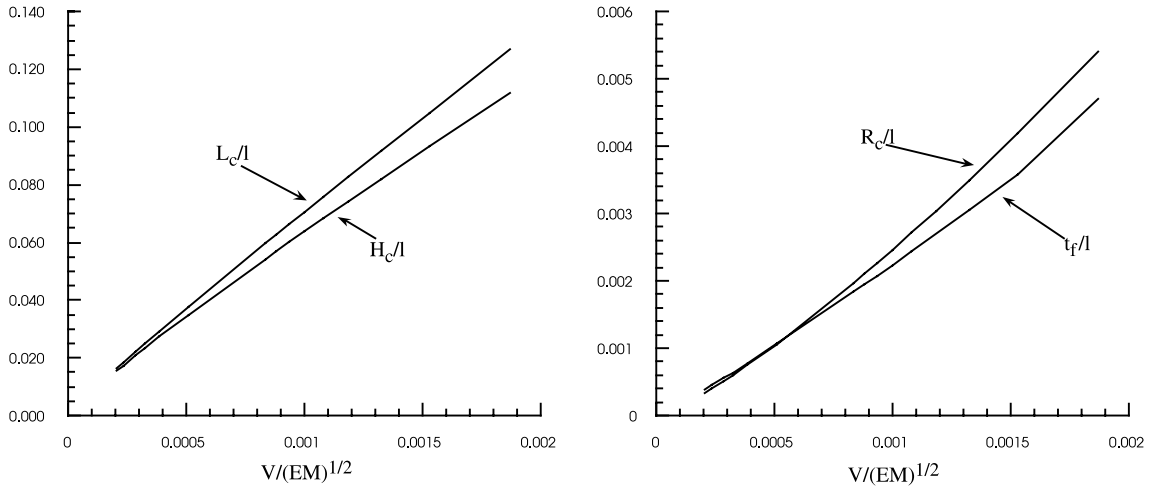

Fig. 8. Face sheet thickness and core member size for the fully optimized sandwich plate ($\sigma_Y/E = 0.007$, $\nu = 1/3$, $k = 1$).

seen in Fig. 9, where both curves have been computed for the unconstrained core geometry. Full clamping is unconservative such that the predicted trend for $W/\rho\ell$ is expected to underestimate the optimal weight of sandwich plates with truss cores. The fact that the spread between the two estimates in Fig. 9 is relatively narrow in spite of the significant difference between the two modeling assumptions suggests that the pinned jointed idealization used in this paper may not give rise to significant error. To the left of the vertical line in Fig. 9, the clamped case has the same three active constraints noted for the case $k = 1$. To the right of the line, all four constraints are active.

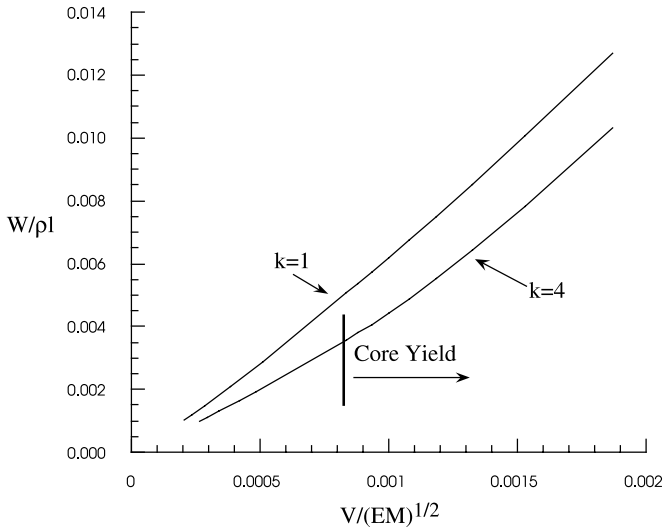

Fig. 9. Comparison of optimal weights of fully optimized sandwich plates with truss cores for two choices of core member end conditions: $k = 1$ (simply-supported) and $k = 4$ (clamped).

4. Weight comparison: truss plates, sandwich plates with truss cores, and honeycomb sandwich plates

Fig. 10 compares the weight per unit area of the fully optimized truss plate of Section 2 and that of the fully optimized sandwich plate with the truss core (with $k = 1$) from Section 3. Included in this plot are the corresponding results for optimized honeycomb sandwich plates, where both the face sheets and the

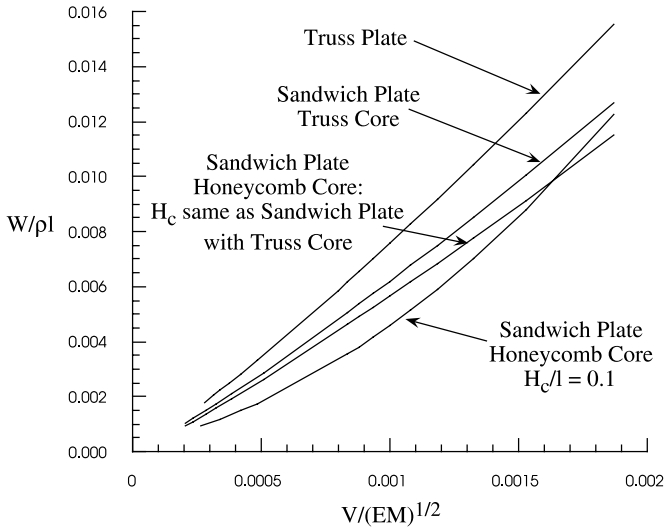

Fig. 10. Comparison of optimal weights of truss plates, sandwich plates with truss cores ($k = 1$), and sandwich plates with honeycomb cores, all with $\sigma_Y/E = 0.007$ and $\nu = 1/3$. The two plates with truss cores are fully optimized. Two cases of the honeycomb plates have been considered: the core thickness fixed at $H_c/\ell = 0.1$; and the core thickness taken equal to that of the sandwich plate with truss core at the same value of $V/\sqrt{EM}$.

honeycomb core are made from the same material as the other two plate structures ($\sigma_Y/E = 0.007$ and $v = 1/3$). As in the case of the other two plate structures, the sole dimensionless loading parameter in the optimization of the honeycomb sandwich is $V^2/(EM)$. The optimization analysis of the honeycomb sandwich is outlined in Appendix A. Four competing failure modes have been considered: face sheet buckling and yielding, and core web buckling and yielding under shear. The four design variables are face sheet thickness, core thickness, web thickness, and the size of the honeycomb hexagon. The fully optimized honeycomb sandwich has a much larger core thickness than either of the two other plate structures analyzed here. So thick, in fact, that the honeycomb sandwich could hardly be considered to be thin and would be unlikely to be a realistic contender. To make a meaningful comparison, two restricted optimization calculations have been performed for the honeycomb sandwich plates. In one, the thickness of the honeycomb sandwich, H_c, was set equal to the thickness of the truss core sandwich plate at the corresponding value of $V^2/(EM)$ (Fig. 8a). In the other calculation, the thickness of the honeycomb plate was set to be $H_c/\ell = 0.1$ over the whole range of $V^2/(EM)$. In each set of calculations, the optimization was then performed with respect to the other three design variables. The outcomes of these restricted optimizations for the honeycomb sandwich are plotted in Fig. 10.

It is striking that the weights of the optimized sandwich plates with truss and honeycomb cores are so similar. Sandwiches with honeycomb cores are generally regarded as the lightest weight plate structures. The comparison of Fig. 10 suggests that truss cores may be equally effective for sandwich plates. Opportunities associated with an open core and possible advantages in face/core bonding may augur well for employment of truss cores.

The optimal weight estimates in Fig. 10 have been determined under approximations to the buckling strengths of each of the three types of plates (e.g. pinned joints and simple supports at joints, where the webs or beam members merge with the faces). All the approximations tend to underestimate the buckling capacity, and thus it is expected that the optimal weight estimates in Fig. 10 are all overestimates. Further work will be required to refine these estimates and to fully certify the relative weight advantages of the three types of plate structures. It seems to us, that of the three types, the design weight of the truss plate is likely to be reduced the most by more accurate buckling analysis. This assertion arises from our expectation that the major error following from the idealization of pinned joints is in the critical load for buckling of the truss faces.

5. Plates with truss cores and solid sheet faces designed as compression panels

The competitive performance under transverse loads of the sandwich plates comprised of solid sheet faces with a truss core motivates their consideration as candidates for compression panels. Here, attention is focused on simply supported wide plates of length, ℓ, designed to carry a prescribed compressive load per unit length, P. (Note that ℓ in this section is defined differently from the previous sections.) In the spirit of a study by Budiansky (1999), the optimal design will be compared with optimally designed stringer stiffened construction, which is among the most efficient for applications requiring light weight. As in the earlier parts of the present study, attention is limited to sandwich plates made from a single material. The structure is the same as that in Section 3, and the notation of that section continues to apply. Specifically, the task in this section is to minimize the weight per unit area (3) of the plate subject to the failure constraints, which now include overall buckling of the plate in the wide column mode. As before, only the loading regime leading to relatively thin plates will be investigated.

Under axial compression P, the face sheets of the unbuckled plate carry all the load such that the forces in the truss members are zero. Yielding or buckling of the individual truss members are no longer limitations on the design. However, the transverse shear stiffness of the core enters into the overall buckling

strength of the plate. The elastic buckling load for a simply supported wide plate of length ℓ having bending stiffness D and transverse shear stiffness S is (Allen, 1969)

$$P_{\text{crit}} = \frac{\pi^2 D}{\ell^2}\left[1 + \frac{\pi^2 D}{\ell^2 S}\right]^{-1}. \tag{23}$$

Only the face sheets contribute to the bending stiffness:

$$D = \frac{1}{2}Et_{\text{f}}(H_{\text{c}} + t_{\text{f}})^2 \cong \frac{1}{2}Et_{\text{f}}H_{\text{c}}^2, \tag{24}$$

where, as in Section 3, it is anticipated that $t_{\text{f}}/H_{\text{c}} \ll 1$, such that the approximation given above can be used. The transverse shear stiffness (which is isotropic) depends on the truss core members according to

$$S = \frac{\pi E R_{\text{c}}^2 H_{\text{c}}^2}{\sqrt{3}L_{\text{c}}^3}. \tag{25}$$

Thus, the overall buckling constraint is

$$P \leqslant P_{\text{crit}}. \tag{26a}$$

There are three other potential failure modes which potentially constrain the design, the first two of which were employed in Section 3. Avoidance of face sheet yielding requires

$$P \leqslant 2\sigma_Y t_{\text{f}}, \tag{26b}$$

while the condition for localized face sheet buckling requires

$$P \leqslant \frac{49}{216}\frac{\pi^2}{(1-\nu^2)}\frac{Et_{\text{f}}^3}{(L_{\text{c}}^2 - H_{\text{c}}^2)}. \tag{26c}$$

The remaining failure mode which must be considered is a compressive kinking mode, which can occur if the transverse shear stiffness is very low. This is a localized mode of buckling, in the order of the thickness of the plate, in which the core shears cause a kink in the centerline of the plate (Allen, 1969). The constraint against kinking is $P \leqslant S$, or, by Eq. (25),

$$P \leqslant \frac{\pi E R_{\text{c}}^2 H_{\text{c}}^2}{\sqrt{3}L_{\text{c}}^3}. \tag{26d}$$

The optimal design problem is the minimization of W in Eq. (3) with respect to t_{f}, L_{c}, R_{c} and H_{c}, subject to the four constraints (26). Again, let $d = \sqrt{L_{\text{c}}^2 - H_{\text{c}}^2}$, and take the vector of dimensionless unknowns to be as defined in Eq. (22). Then, the problem becomes the minimization of the dimensionless weight per area

$$W/(\rho\ell) = 2\left[x_1 + \pi x_2^2\sqrt{x_3^2 + x_4^2}/(\sqrt{3}x_4^2)\right], \tag{27}$$

subject to the four constraints:

$$\left(\frac{P}{E\ell}\right)\frac{2}{\pi^2}x_1^{-1}x_3^{-2}\left[1 + \frac{\sqrt{3}\pi}{2}x_1\left(x_3^2 + x_4^2\right)^{3/2}/x_2^2\right]^{-1} \leqslant 1, \text{ (overall buckling)}, \tag{28a}$$

$$\frac{1}{2}\left(\frac{P}{E\ell}\right)\left(\frac{E}{\sigma_Y}\right)x_1^{-1} \leqslant 1, \text{ (face sheet yielding)}, \tag{28b}$$

$$\left(\frac{P}{E\ell}\right)\frac{216(1-\nu^2)}{49\pi^2}x_1^{-3}x_4^2 \leqslant 1, \text{ (face sheet buckling)}, \tag{28c}$$

$$\left(\frac{P}{E\ell}\right)\frac{\sqrt{3}}{\pi}x_2^{-2}x_3^{-2}\left(x_3^2+x_4^2\right)^{3/2} \leqslant 1, \text{ (localized kinking)}. \tag{28d}$$

The prescribed dimensionless load parameter is $P/(E\ell)$, and the two material parameters are σ_Y/E and ν.

The outcome of the optimization analysis is shown in Figs. 11 and 12 for $\sigma_Y/E = 0.007$ and $\nu = 1/3$. Both the full optimization with respect to the four variables and the geometrically constrained optimization are included with $H_c = \sqrt{2/3}L_c$, corresponding to the same tetrahedral core geometry considered in Sections 2 and 3. The range of the load parameter has been chosen to be consistent with the stated condition

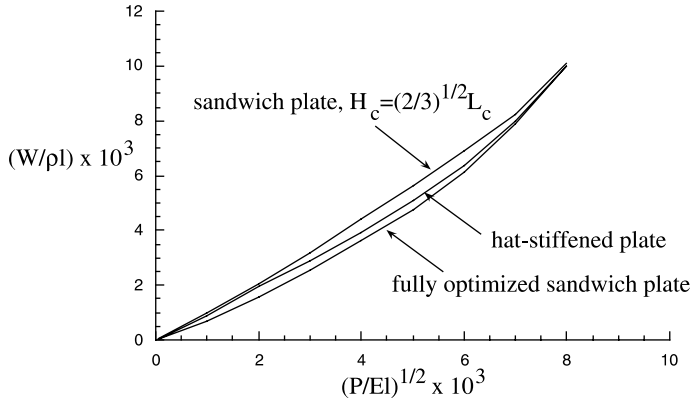

Fig. 11. Normalized weight per unit area as a function of the dimensionless load parameter for optimally designed simply-supported wide panels under axial compression ($\sigma_Y/E = 0.007$ and $\nu = 1/3$). The upper and lower curves are for the sandwich plates with a truss core, constrained with $H_c = \sqrt{2/3}L_c$ and unconstrained, respectively. The middle curve is an optimized hat-stiffened single layer plate, which is regarded as one of the most efficient structures for this application.

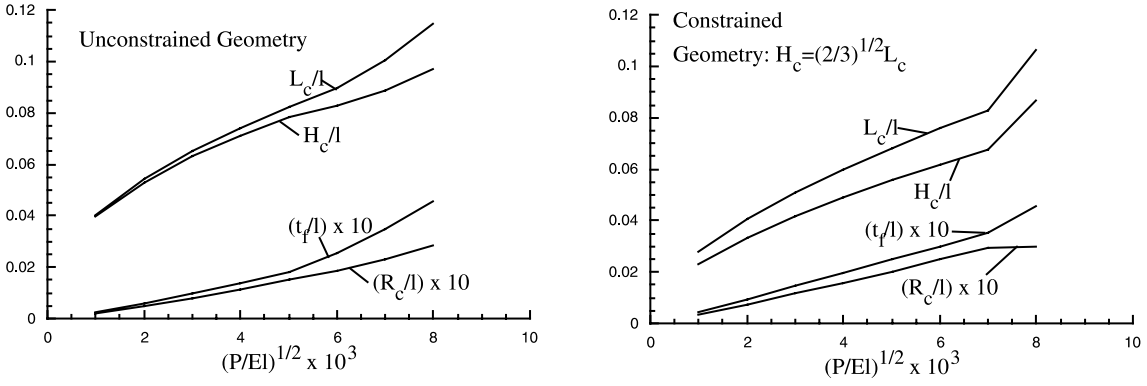

Fig. 12. Normalized variables specifying the optimal truss core sandwich plates in Fig. 11: (a) unconstrained case and (b) constrained case ($H_c = \sqrt{2/3}L_c$).

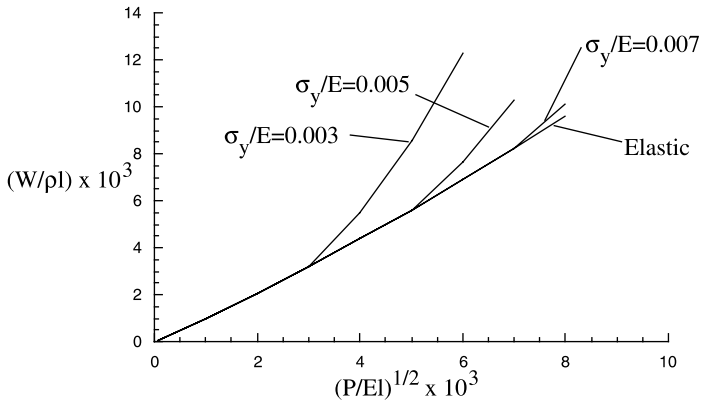

Fig. 13. Normalized weight per unit area for truss core sandwich plates with constrained geometry ($H_c = \sqrt{2/3}L_c$) for strictly elastic designs and for three values of σ_Y/E, all with $\nu = 1/3$.

that the plate be relatively thin. Plots of the design variables for the optimum plates are displayed in Fig. 12 revealing that H_c/ℓ approaches 1/10 at the upper end of the range of the load parameter plotted. The kinking mode is never active over the entire range of the load parameter considered. The more heavily loaded compression panels have three of the constraints active in the optimal design: overall and face sheet buckling and face sheet yielding. More lightly loaded panels (below the jump in the slope of the curves) buckle at the design load simultaneously in the overall and localized face sheet modes, but are stressed below yield.

Included in Fig. 11 as a standard for evaluating the performance of the optimal truss core sandwich plates is the weight for an optimal hat-stiffened plate (Budiansky, 1999), also with $\sigma_Y/E = 0.007$ and $\nu = 1/3$. Hat-stiffened plates are generally regarded to be one of the most efficient light weight constructions for compression panels. The unconstrained truss core sandwich plates are lighter than the hat-stiffened plates, while the constrained design is only slightly heavier.

The results for the more lightly loaded optimal panels buckle below yield and therefore depend only on the elastic moduli. However, the upper limit of $P/(E\ell)$ for strictly elastic design depends on σ_Y/E. Fig. 13 presents the weight per unit area as a function of the load parameter for three values of σ_Y/E for optimized compression sandwich plates with truss cores. These results are for plates with cores subject to the geometric constraint $H_c = \sqrt{2/3}L_c$, but results for the fully optimized panels follow the same trend. The weight of the more heavily loaded panels increases sharply with decrease in yield strength material.

Acknowledgements

This work was supported in part by grants ONR-N00014-1-96-1028 and NSF-DMR-98-09363 and in part by the Division of Applied Sciences, Harvard University. Nathan Wicks acknowledges the fellowship support of the National Defense Science and Engineering Graduate Fellowship Program.

Appendix A. Optimized honeycomb sandwich plates

Sandwich plates with honeycomb cores are used in Fig. 10 to gauge the performance of the truss plates and the sandwich plates with truss cores. The faces and the honeycomb core are assumed to be made of the

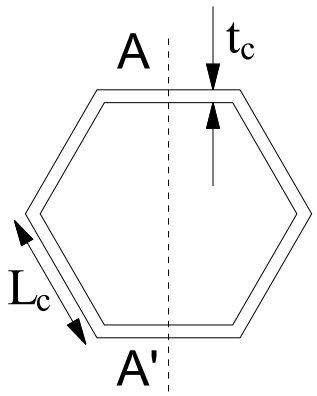

Fig. 14. Conventions for honeycomb core analysis.

same material, as was the case of the other two structures. The face sheet thickness is t_f, the core thickness is H_c, the thickness of the honeycomb web is t_c, and the length of each side of the honeycomb hexagon is L_c. The weight per unit area is

$$W = \rho\left(\frac{2H_c t_c}{\sqrt{3}L_c} + 2t_f\right). \tag{A.1}$$

The analysis follows that of the truss core sandwich fairly closely, with similar approximations. The maximum moment per unit length and transverse shear force per unit length are again denoted by M and V and oriented parallel to the section A–A' in Fig. 14. The transverse shear force is assumed to be carried entirely by the honeycomb core. Under these assumptions, the stress in the face sheet is

$$\sigma_f = \frac{M}{t_f H_c}, \tag{A.2}$$

while the average shear stress in the core web oriented perpendicular to the load line is

$$\tau_c = \frac{\sqrt{3}VL_c}{t_c H_c}. \tag{A.3}$$

The weight per unit area is minimized subject to the following four strength constraints:

$$\frac{M}{t_f H_c} \leqslant \sigma_Y, \text{ (face sheet yielding)}, \tag{A.4}$$

$$\frac{M}{t_f H_c} \leqslant \frac{379\pi^2 E t_f^2}{1728(1-\nu^2)L_c^2}, \text{ (face sheet buckling)}, \tag{A.5}$$

$$\frac{\sqrt{3}VL_c}{t_c H_c} \leqslant \tau_Y, \text{ (core web yielding)}, \tag{A.6}$$

$$\begin{aligned} \frac{\sqrt{3}VL_c}{t_c H_c} &\leqslant \frac{\pi^2 E}{12(1-\nu^2)}\left[5.35\frac{t_c^2}{H_c^2} + 4\frac{t_c^2}{L_c^2}\right], \quad \text{if } L_c > H_c \\ &\leqslant \frac{\pi^2 E}{12(1-\nu^2)}\left[5.35\frac{t_c^2}{L_c^2} + 4\frac{t_c^2}{H_c^2}\right], \quad \text{if } H_c > L_c, \end{aligned} \quad \text{(core web buckling)}, \tag{A.7}$$

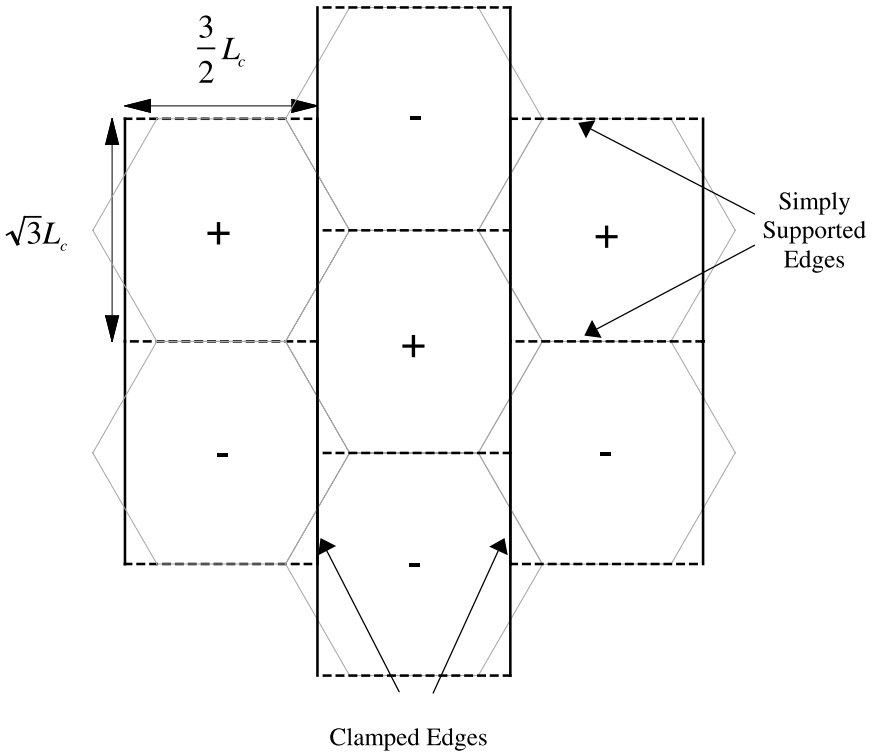

Fig. 15. Nodal lines for face sheet buckling mode for sandwich plates with honeycomb core. The compression direction is horizontal. To comply with the constraint of the core geometry, simple support conditions are taken along the horizontal nodal lines, and clamped conditions are assumed along the vertical nodal lines.

where $\tau_Y = \sigma_Y/\sqrt{3}$. The face sheet buckling mode is approximated by a rectangular pattern with dimensions $3L_c/2$ by $\sqrt{3}L_c$ and clamped on the edges parallel to the load line and simply supported on the edges perpendicular to the load line. This choice was made to model the constraint of the honeycomb core on the sheet buckling mode, as indicated in Fig. 15. The average shear stress in the core is equated to the yield stress in shear to determine (A.6). Core buckling is assumed to be associated with a plate subject to uniform shear τ_c of dimension L_c by H_c and simply supported on all its edges (Timoshenko and Gere, 1961). The simple support conditions underestimate the rotational constraint of the adjoining webs and the face sheets.

When cast into dimensionless variables in the manner of the previous sections, the only load parameter is $V/\sqrt{EM}$ and the material parameters are σ_Y/E and v. Computations minimizing the weight subject to the four constraints have been carried out for $\sigma_Y/E = 0.007$ and $v = 1/3$. Over the entire range of the loading parameter considered in this paper, the value H_c/ℓ of associated with the optimum was greater than 0.15. This is not a thin plate and it is highly unlikely that such a plate would be considered in an application. To make a meaningful comparison between the honeycomb core sandwich and the other plate structures, two different constraints on H_c were considered: (i) H_c/ℓ was fixed at 0.1 for all values of $V/\sqrt{EM}$ and (ii) H_c/ℓ was taken to be same as H_c/ℓ for the fully optimized truss core sandwich plate at each value of $V/\sqrt{EM}$. In each of these two cases, the honeycomb core sandwich was then optimized with respect to the remaining three variables. The results are shown in Fig. 10. Over the entire range of the load parameter plotted, the optimal honeycomb core sandwich exhibits simultaneous face sheet yielding, face sheet buckling and core buckling.

References

Allen, H.G., 1969. Analysis and Design of Structural Sandwich Panels. Pergamon Press, Oxford.

Brittain, S.T., Sugimura, Y., Schueller, J.A., Evans, A.G., Whitesides, G.M., 2000. Fabrication of a mesoscale, space-filling truss system using soft lithography and microelectrochemistry, submitted for publication.

Budiansky, B., 1999. On the minimum weights of compression panels. Int. J. Solids Struct. 36, 3677–3708.

Fuller, R.B., 1983. Octet truss (1961) in inventions, St. Martins Press, New York, pp. 167–177.

Timoshenko, S.P., Gere, J.M., 1961. Theory of elastic stability. McGraw-Hill, New York.

Wallach, J.C., Gibson, L.G., 2000. Mechanical behaviour of a three-dimensional truss material. Int. J. Solids Struct. submitted for publication.